Journal Of Research Technology & Engineering
www.jrte.org

Green Synthesis of Zinc Oxide Nanoparticles for Biocompatible and Sustainable Sunscreens with Enhanced UV Protection and Antibacterial Activity

*[1]K.A.P.N. Kumari, [2]K.H.I.K. Hewavitharana

[1]Department of Biosystems Technology, Faculty of Technological Studies, Uva Wellassa University of Sri Lanka.
[2]Department of Biosystems Technology, Faculty of Technological Studies, Uva Wellassa University of Sri Lanka
*poornimanilupa66@gmail.com

Received:28 Feb 2025; Revised: 22 Mar 2025; Accepted: 30 Mar 2025; Available online: 10 Apr 2025

Abstract— Sunscreens play a critical role in protecting the skin from harmful ultraviolet (UV) radiation, including both UVA and UVB rays. Traditional inorganic UV filters, such as chemically synthesized zinc oxide (ZnO) and titanium dioxide (TiO_2), have limitations regarding biocompatibility, cost, and sustainability. This study investigates the effectiveness of green-synthesized ZnO nanoparticles (NPs) as an alternative, focusing on their potential for UV attenuation in sunscreens. ZnO NPs were synthesized using zinc acetate dihydrate as a precursor, and green synthesis was performed with leaf extracts from *Talinum fruticosum* and *Sauropus androgynus*, plants rich in bioactive phytochemicals like flavonoids, alkaloids, and phenolic compounds, enhancing the nanoparticles' antioxidant, antimicrobial, and anti-inflammatory properties. Sunscreens were formulated by incorporating ZnO NPs at 5%, 15%, and 25% concentrations into a cream base. Characterization of the nanoparticles was conducted using Fourier Transform Infrared (FT-IR) spectroscopy, X-ray diffraction (XRD), and UV-Vis spectroscopy. XRD analysis confirmed the successful formation of nanoparticles, with crystallite sizes of 13.31 nm for chemically synthesized ZnO and 16.82–16.83 nm for the green-synthesized ZnO. UV-Vis spectroscopy revealed absorption peaks at 365 nm for *Talinum fruticosum* and 364 nm for *Sauropus androgynus* ZnO NPs, compared to 363 nm for the chemically synthesized ZnO. The green-synthesized ZnO NPs exhibited superior UV absorption, antioxidant, and antibacterial properties, with the 25% concentration of *Talinum fruticosum* ZnO NPs proving most effective. Overall, green-synthesized ZnO NPs demonstrated enhanced UV protection compared to their chemically synthesized counterparts, providing a more sustainable and functional alternative for sunscreen formulations.

Keywords: Antioxidant Properties; Biocompatible Sunscreen; Sustainable Green Nanomaterials; Sunscreen Formulations; UV Protection; Zinc Oxide Nanoparticles.

1 INTRODUCTION

Skin is the largest organ of the human body and protecting it from ultraviolet (UV) radiation is essential. UV exposure from the sun can cause both acute and chronic harm, leading to conditions such as sunburn, photocarcinogenesis (skin cancer), photo immunosuppression (weakened immune response), and photoaging (premature aging of the skin). UV radiation is divided into three types: UVA, UVB, and UVC. UVC radiation

is not harmful to the skin as it is absorbed by the ozone layer. UVA (320–400 nm) has a longer wavelength, allowing it to penetrate deeper into the skin, while UVB (290–320 nm) has shorter wavelengths and is primarily responsible for causing DNA damage in the epidermis. Current methods of photoprotection include sun avoidance, seeking shade, wearing protective clothing, and applying sunscreen. Among these, sunscreen is the most commonly used and effective means of protecting the skin from harmful UV radiation. Sunscreens contain UV filters, which are categorized into two types: chemical and physical. Chemical UV filters absorb UV radiation, but they can sometimes cause skin irritation, allergic reactions, or photoallergic contact dermatitis. Physical (or inorganic) UV filters, such as titanium dioxide (TiO_2) and zinc oxide (ZnO), work by reflecting or scattering UV radiation. While TiO_2 is a widely used physical filter, it can be relatively expensive. ZnO, on the other hand, is a cost-effective and efficient alternative, offering protection against both UVA and UVB radiation. ZnO can also be synthesized into nanoparticles, which enhance its efficacy in sunscreens by improving dispersion and increasing surface area.

ZnO nanoparticles can be synthesized using various methods, such as sol-gel, hydrothermal synthesis, vapor deposition, spray pyrolysis, and thermal decomposition. However, a novel approach known as green synthesis has gained attention due to its eco-friendly and sustainable nature. In this method, plant extracts rich in reducing agents are used to reduce metal salts into nanoparticles. The green synthesis of ZnO nanoparticles offers several advantages, including control over particle size, shape, and uniformity, as well as the use of non-toxic, natural reagents. Plant-based synthesis of ZnO nanoparticles aligns with the growing trend of green chemistry, which emphasizes sustainability and environmental safety. In this approach, plant parts like leaves, flowers, roots, and peels are used for nanoparticle production, reducing the need for harmful chemicals. This study focuses on synthesizing ZnO nanoparticles using the leaves of *Sauropus androgynus* (Sweet Leaf) and *Talinum fruticosum* (Ceylon spinach). Both plants are rich in zinc, as well as possessing antioxidant, antibacterial, and UV-protective properties, making them ideal candidates for biosynthesis [1], [2], [3]

2 METHODOLOGY

2.1 ZnO nanoparticle Synthesis

2.1.1 Chemical Synthesis of ZnO Nanoparticles.

A 0.02 M aqueous solution of zinc acetate dihydrate was prepared by dissolving the compound in 50 mL of distilled water under vigorous stirring. At room temperature, 2.0 M sodium hydroxide (NaOH) was added drop by drop to adjust the pH to 12. The solution was then stirred continuously for 2 hours. After the reaction, the resulting white precipitate was washed thoroughly with distilled water, followed by ethanol, to remove impurities. The precipitate was then dried in a vacuum oven at 60°C overnight. (Fig.1.)

2.1.2 Green synthesis of ZnO Nanoparticles

2.1.2.1 Preparation of Leaf Extracts

2.1.2.1.1 *Talinum fruticosum* Leaf Extract Preparation:

The leaves of *Talinum fruticosum* (Ceylon spinach) were thoroughly washed with distilled water to remove dust and contaminants. The cleaned leaves were then air-dried at room temperature and ground into a fine

powder. A 5 g sample of the leaf powder was added to 50 mL of distilled water and boiled for 2 hours at 60°C, while stirring at 60 rpm using a magnetic stirrer. After boiling, the leaf extract was filtered through Whatman filter paper and stored in a refrigerator for future use.

2.1.2.1.2 *Sauropus androgynus* Leaf Extract Preparation:

Similarly, the leaves of *Sauropus androgynus* (Sweet leaf) were washed with distilled water, air-dried, and ground into powder. A 5 g sample of leaf powder was added to 50 mL of distilled water and boiled at 60°C for 2 hours with constant stirring at 60 rpm. After boiling, the extract was filtered using Whatman filter paper and stored at 4°C for future use.

2.1.2.2 Green synthesis of ZnO Nanoparticles from *Talinum fruticosum* Extract

A 0.02 M aqueous solution of zinc acetate dihydrate was prepared by dissolving the compound in 50 mL of distilled water under constant stirring. After 10 minutes, 1 mL of the *Talinum fruticosum* leaf extract was added to the solution. Sodium hydroxide (NaOH) (2.0 M) was then added dropwise to adjust the pH to 12, resulting in a pale white solution. The reaction mixture was stirred for 2 hours, after which the pale white precipitate was collected. The precipitate was washed three times with distilled water, followed by ethanol, to remove impurities. Finally, the ZnO nanoparticles were obtained as a pale white powder after drying at 60°C in a vacuum oven overnight (Fig. 1.).

2.1.2.3 Green synthesis of ZnO Nanoparticles from *Sauropus androgynus* Extract

A 0.02 M aqueous solution of zinc acetate dihydrate was prepared in 50 mL of distilled water and stirred continuously. After 10 minutes, 1 mL of *Sauropus androgynus* leaf extract was added to the solution. Sodium hydroxide (2.0 M) was then added dropwise to bring the pH to 12, forming a pale white solution. The mixture was stirred for 2 hours, and the resulting precipitate was collected, washed thoroughly with distilled water, followed by ethanol to remove any impurities. The ZnO nanoparticles were obtained as a pale white powder after drying in a vacuum oven at 60°C overnight. (Fig.1.)

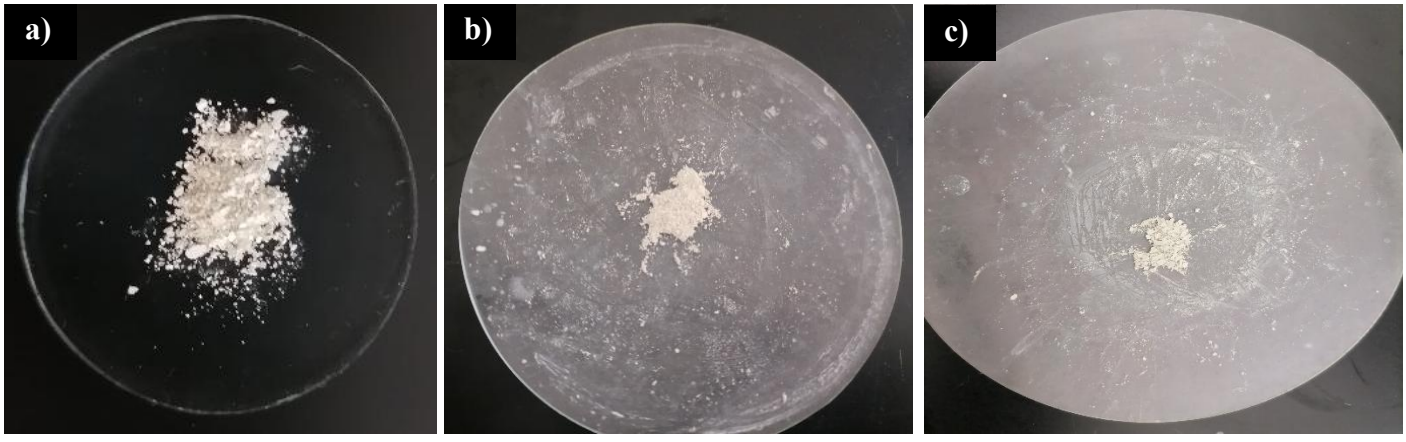

Fig. 1. a) Chemically synthesized ZnO NPs b) *Tallinum fruticosum* synthesized ZnO NPs and c) *Sauropus androgynus* synthesized ZnO NPs

2.2 Sunscreen development

3 grams of sunscreen were prepared by mixing chemically and green synthesized ZnO nanoparticles with a cream base using a vortex mixer for 15 minutes at room temperature. The weights of ZnO nanoparticles and the cream base used for the preparation of 3 grams of sunscreen are mentioned in Table 1. In this study, 09 Sunscreen samples were prepared by mixing 5%, 15%, and 25% (w/w) ZnO nanoparticles with the cream base (Fig. 2.).

Table 1: Sunscreen Preparation using ZnO NPs & Cream base mixture

Sunscreen Sample		5% Sunscreen	15% Sunscreen	25% Sunscreen
ZnO NPs Weight	Chemically synthesis ZnO NPs	0.15	0.45g	0.75g
	Green Synthesis of ZnO NPs from *Talinum fruticosum*	0.15	0.45g	0.75 g
	Green Synthesis of ZnO NPs from *Sauropus androgynus*	0.15	0.45 g	0.75 g
Cream Base Weight (g)		2.85	2.55	2.25

Fig. 2. a) Chemically synthesized ZnO NPs Sunscreen samples b) *Talinum fruticosum* synthesized ZnO NPs sunscreen samples c) *Sauropus androgynus* synthesized ZnO NPs sunscreen samples

2.3 ZnO Nanoparticle Characterization

2.3.1 UV-Vis Spectrophotometric Analysis of ZnO NPs

Chemically synthesized and green synthesized ZnO nanoparticles (0.1 g each) were dissolved in 5 mL of distilled water to achieve a concentration of 20 mg/mL. The solution was mixed using a vortex mixer. Absorbance spectra were recorded in the range of 200–800 nm using a UV-Vis spectrophotometer (6137KG005002, Germany).

2.3.2 FT-IR Spectroscopic Analysis

The molecular structure of the chemically and Green synthesized ZnO nanoparticles was characterized using a Fourier-transform infrared (FTIR) spectrophotometer (201113, Germany) in the wavenumber range of 4000–400 cm^{-1}

2.3.3 XRD Analysis

The crystalline structure and particle size of the synthesized ZnO nanoparticles were analyzed by X-ray diffraction (XRD) using a Miniflex 600 diffractometer (Rigaku Corporation, Japan) [4].

2.4 Sunscreen Evaluation

2.4.1 UV-Vis Absorption Analysis

A blank solution was prepared by mixing 5 mL of methanol and 5 mL of distilled water. 1 g of sunscreen was added to a beaker, and 5 mL of the stock solution was transferred into a new container. The sample was diluted three times (1:2 ratio of sample to blank), and the absorption was measured in the range of 220–400 nm using a UV-Vis spectrophotometer (6137KG005002, Germany).

2.4.2 Antibacterial Properties Evaluation of Sunscreen

The antibacterial activity of sunscreens prepared with chemically synthesized and green synthesized ZnO nanoparticles (at concentrations of 5% and 25%) was evaluated using the disk diffusion method [5]. The bacterial strains *Staphylococcus aureus* (MTCC 7443, gram-positive) and *Escherichia coli* (MTCC 7410, gram-negative) were obtained from the Microbial Type Culture Collection (Medical Research Institute, Sri Lanka). The bacteria were sub-cultured and maintained on nutrient agar medium.

2.4.2.1 Preparation of Working Culture Plates:

Nutrient agar (NA) plates, inoculation loops, and petri dishes were sterilized at 121°C for 15 minutes. Under sterile conditions, the sterilized NA was poured into petri plates and allowed to solidify overnight. After solidification, the pure bacterial strains were streaked onto the agar using an inoculation loop and incubated at 28°C for 24 hours.

2.4.2.2 Barium Sulfate ($BaSO_4$) Turbidity Standard Preparation:

In a test tube, 0.05 mL of a 1% $BaCl_2$ solution was added to 9.95 mL of sulfuric acid, and the solutions were mixed thoroughly to form barium sulfate with the desired turbidity level.

2.4.2.3 Generation of Bacterial Suspension and Colony Counts:

Bacterial colonies were isolated from NA plates, and 3–5 colonies were transferred to a test tube containing 10 mL of distilled water. The solution was vortexed to mix evenly. The optical density of the suspension was adjusted to match the 0.5 McFarland standard, corresponding to 1.5×10^8 CFU/mL.

2.4.2.4 Antibacterial Properties Evaluation of Sunscreen

The antimicrobial activity of the sunscreens was assessed using the disk diffusion method. Nutrient agar was poured into sterilized Petri dishes and allowed to solidify. After solidification, 0.1 mL of bacterial suspension corresponding to the 0.5 McFarland standard was evenly spread over the surface of the agar plates. Sterile forceps were used to place the antibiotic-impregnated discs onto the agar surface. The plates were incubated at 37°C for 24 hours. After incubation, the zone of inhibition around each disc was measured using a ruler. The controls included discs soaked in amoxicillin (positive control) and distilled water (negative control), which served as a comparison for the antimicrobial efficacy of the sunscreen formulations. The sunscreen formulations tested included those with ZnO nanoparticles synthesized from *Sauropus androgynus* (Sweet Leaf), *Talinum fruticosum* (Ceylon Spinach), and chemically synthesized ZnO. The discs were labeled as A: Positive control (Amoxicillin), B: Sunscreen with Sweet Leaf-synthesized ZnO, C: Sunscreen with

Ceylon Spinach-synthesized ZnO, D: Sunscreen with chemically synthesized ZnO, E: Negative control (Distilled water)

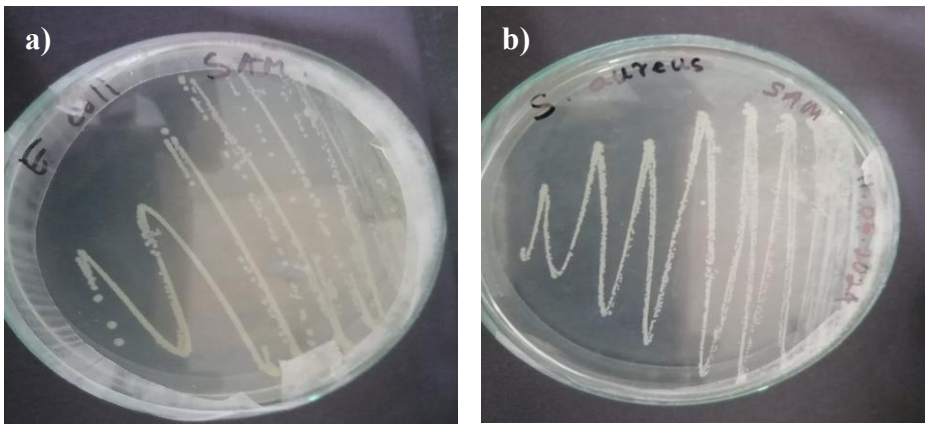

Fig. 3. a) *E. coli* Working culture and b) *S. aureus* Working culture

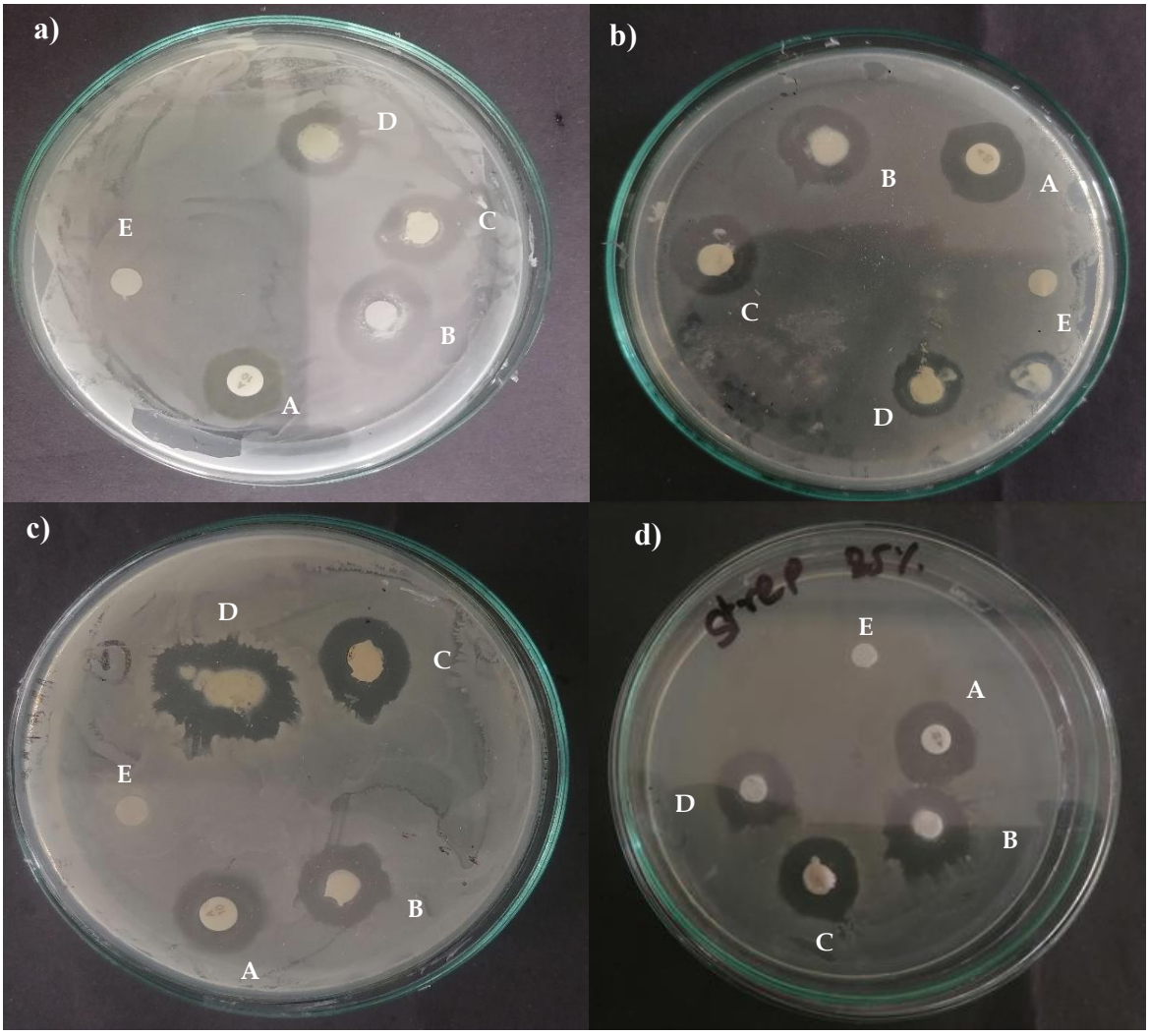

Fig. 4. a) Inhibition zone for 5% concentration Sunscreen samples for *E. coli,* b) Inhibition zone for 5% concentration Sunscreen samples for *S. aureus,* c) Inhibition zone for 25% concentration Sunscreen samples for *E. coli*, and d) Inhibition zone for 25% concentration Sunscreen samples for *S. aureus*

2.4.3 Antioxidant Properties

2.4.3.1 Determination of Total Antioxidant Capacity (DPPH Radical Scavenging Assay)

2.4.3.1.1 Stock Solution Preparation:

4 mg of the sunscreen sample was weighed and dissolved in 4 mL of methanol. The solution was shaken and covered with aluminum foil to protect it from light.

2.4.3.1.2 DPPH Solution Preparation:

To prepare a 1 mM DPPH solution, 4 mL of DPPH was mixed with 100 mL of 99% methanol. The flask was covered with aluminum foil and stored in the dark to avoid degradation of the DPPH.

2.4.3.1.3 Sunscreen Antioxidant Preparation:

After 1 hour of preparation, sunscreen samples were prepared in series with the following volumes: 100 µL, 150 µL, 200 µL, 250 µL, and 300 µL. Each volume was made up to a final volume of 4 mL with 99% methanol and shaken thoroughly. 1 mL of each prepared sample was transferred to separate test tubes, and 3 mL of the DPPH solution was added to each. The test tubes were covered with aluminum foil and kept in the dark for 30 minutes. The absorbance of each sample was then measured at 517 nm using a UV-Vis spectrophotometer.

2.4.3.1.4 Ascorbic Acid Preparation:

For the positive control, ascorbic acid (standard antioxidant) was prepared by dissolving 4 mL of ascorbic acid in 4 mL of methanol. The solution was shaken and covered with aluminum foil.

2.4.3.1.5 Ascorbic Acid Antioxidant Activity:

After 1-hour, ascorbic acid samples were prepared in the same series of volumes: 100 µL, 150 µL, 200 µL, 250 µL, and 300 µL. Each sample was made up to 4 mL with 99% methanol and shaken well. 1 mL from each sample was transferred to separate test tubes, and 3 mL of DPPH solution was added to each. The test tubes were covered with aluminum foil and kept in the dark for 30 minutes. The absorbance was then measured at 517 nm using a UV-Vis spectrophotometer.

2.4.3.1.6 Calculation of Radical Scavenging Activity

The percentage of inhibition (scavenging activity) was calculated using the following formula:

$$\text{Inhibition \%} = (\text{Control Absorbance} - \text{Sample Absorbance})/\text{Control Absorbance} \times 100$$

Where:

Control Absorbance refers to the DPPH solution without the sample (blank).

Sample Absorbance refers to the absorbance measured for the sample with the DPPH solution.

2.5 Statistical Analysis

The antibacterial activity, based on the inhibition zone, was recorded and analyzed using Tukey's pairwise comparison method in MINITAB statistical software version 17.0. A significance level of $\alpha = 5\%$ was used for all comparisons.

2.6 Data Analysis

Data from the X-ray diffraction (XRD), Fourier-transform infrared (FTIR), and UV-Vis analyses were processed using OriginPro 2024b (64-bit version). Graphs were plotted to visually represent the data.

3 Results and Discussion

3.1 ZnO NPs Characterization

3.1.1 XRD Analysis (X-Ray Diffraction)

The crystalline nature and particle size of the synthesized ZnO nanoparticles (NPs) were characterized using a Powder X-ray diffractometer (Chandra, Singh, and Kumari, 2015). For the chemically synthesized ZnO NPs, peaks were identified at 31.45°, 34.1°, 36.0°, 58.25°, 62.65°, and 67.8°. For ZnO NPs synthesized from Sweet Leaf, peaks were observed at 31.25°, 33.85°, 36.7°, 47°, 58°, 62.3°, and 67.5°. For the Ceylon Spinach-synthesized ZnO NPs, peaks appeared at 31.25°, 33.9°, 35.75°, 58.05°, 62.35°, and 67.45°. The average crystallite size of the chemically synthesized ZnO NPs was 13.31 nm, while the crystallite sizes of the Sweet Leaf and Ceylon Spinach ZnO NPs were 16.82 nm and 16.83 nm, respectively. The crystallite size was calculated using Scherrer's formula. Results indicated that the ZnO nanoparticles were in the nano-range, and enhances the UV scattering properties of ZnO, which is beneficial for applications such as sunscreens. No peaks related to impurities were observed, indicating the pure ZnO nature of the synthesized nanoparticles (Kajbafvala et al., 2009). The sharp and intense diffraction peaks confirm the high crystallinity of the nanoparticles.

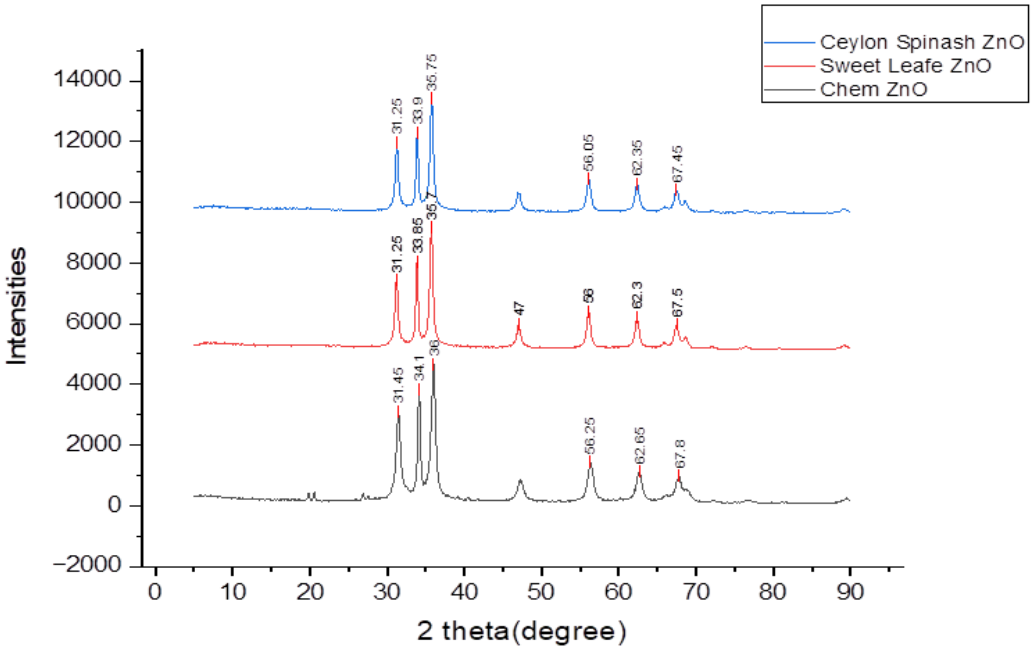

Fig. 5. XRD spectrum for chemically and green synthesized ZnO NPs

3.1.2 FTIR Analysis (Fourier Transform Infrared Spectroscopy)

FTIR spectroscopy was used to identify the functional groups and interactions on the surface of the synthesized ZnO nanoparticles. Spectra for all three samples (chemically synthesized ZnO, Ceylon Spinach ZnO, and Sweet Leaf ZnO) were recorded in the range of 4000 cm^{-1} to 400 cm^{-1}. In the chemically synthesized ZnO sample, a broad peak at 3370 cm^{-1} corresponded to O-H stretching vibrations, suggesting the presence of hydroxyl groups or surface-bound water on the ZnO nanoparticles. Peaks at 2330.90 cm^{-1} and 2084.20 cm^{-1} were attributed to atmospheric CO_2 adsorption, while peaks at 1433 cm^{-1} were associated with C-H bending vibrations, indicative of trace organic residues from the synthesis process. Peaks at 908 cm^{-1}, 842 cm^{-1}, 705.65 cm^{-1}, 634.60 cm^{-1}, and 513.53 cm^{-1} corresponded to Zn-O stretching vibrations, confirming the formation of ZnO nanoparticles. For the Ceylon Spinach-synthesized ZnO, the broad absorption band at 3377 cm^{-1} was attributed to O-H stretching, indicating the presence of hydroxyl groups or hydrophilic components. Additional peaks at 2926 cm^{-1} and 1730 cm^{-1} (C-H and C=O stretching vibrations, respectively) suggested the presence of aliphatic hydrocarbons and carbonyl groups from the spinach extract, which may interact with ZnO. Peaks at 1022.00 cm^{-1} indicated C-O stretching, indicating various oxygenated functional groups that could stabilize the ZnO nanoparticles. In the Sweet Leaf-synthesized ZnO, a broad O-H stretching peak appeared at 3394 cm^{-1}, while C-H stretching peaks were found at 2916.19 cm^{-1}, indicating the presence of organic compounds in the extract. Peaks at 1644 cm^{-1} and 1498 cm^{-1} were attributed to C=O stretching and C-H bending, respectively, suggesting that the extract contains carbonyl groups and aliphatic components. The Zn-O stretching vibrations observed around 887 cm^{-1} further confirmed the presence of ZnO nanoparticles.

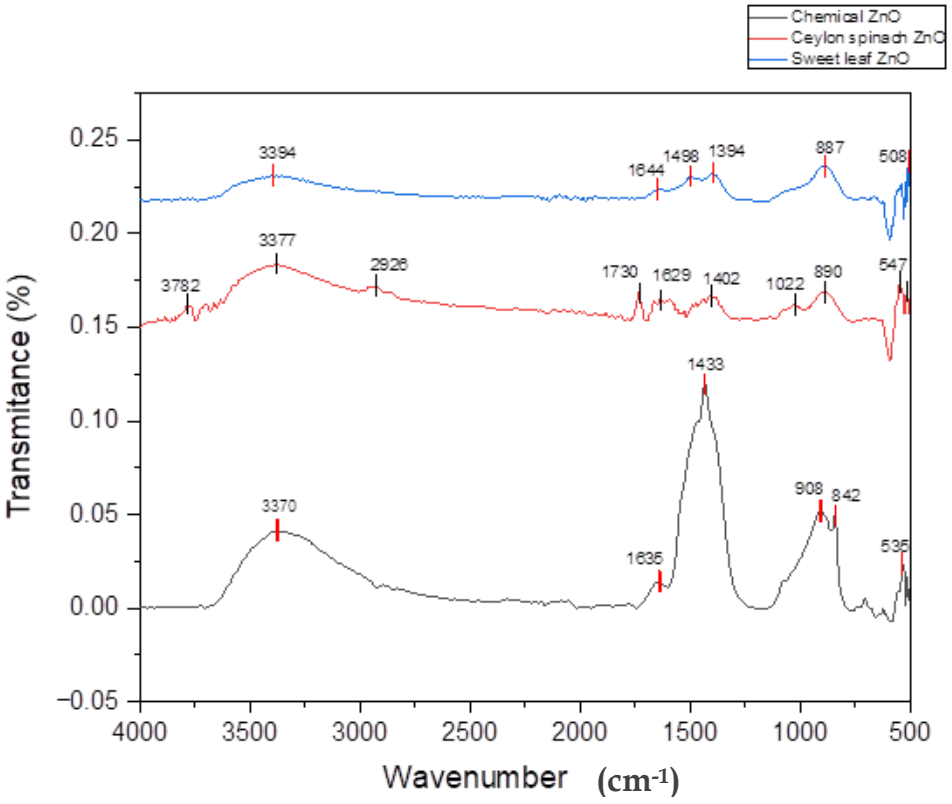

Fig. 6. FTIR graph for chemically and green synthesized ZnO NPs

3.1.3 UV-Vis Spectroscopy

UV–visible diffuse reflectance spectra of ZnO NPs from Sweet Leaf, Ceylon Spinach, and chemically synthesized ZnO NPs were recorded from 220 to 800 nm. Figure 16 presents the UV-vis absorption spectra. The chemically synthesized ZnO NPs displayed low reflectance throughout the UV spectrum (200–800 nm), particularly across the UV-B (280–320 nm) and UV-A (320–400 nm) regions. In contrast, the green synthesized ZnO NPs from Sweet Leaf and Ceylon Spinach exhibited higher reflectance values, with notable absorption peaks around 360 nm and 381 nm, indicating enhanced UV protection, especially against UV-B and part of UV-A rays.

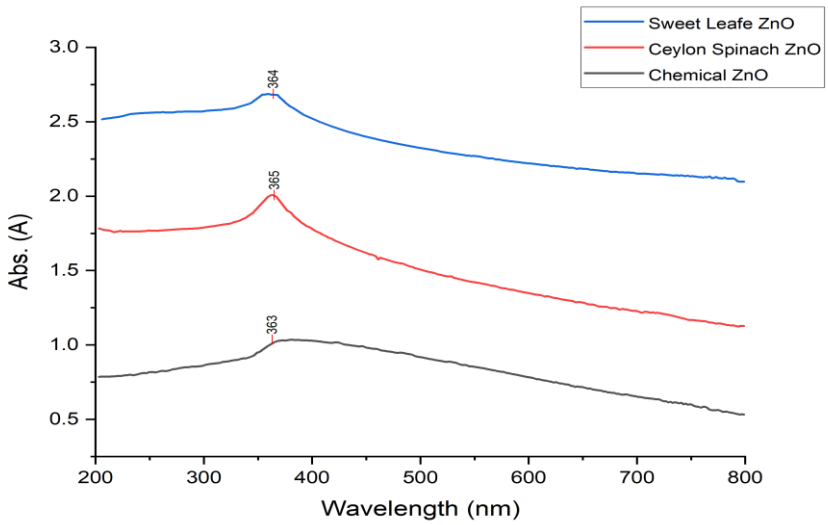

Fig. 7. Uv-vis spectrum of chemically and green synthesized ZnO NPs

3.2 Sunscreen Evaluation

3.2.1 Antioxidant Activity (IC50 Value) of Sunscreen

The IC50 values, indicating the antioxidant activity of the sunscreen formulations with different ZnO NP concentrations (5%, 15%, 25%), are summarized in Table 3. The IC50 values varied depending on the ZnO nanoparticle synthesis method and concentration. Chemically synthesized ZnO NPs: IC50 values of 425.92 µg/ml (5%), 416.44 µg/ml (15%), and 276.92 µg/ml (25%). Ceylon Spinach ZnO NPs: IC50 values of 240.52 µg/ml (5%), 235.69 µg/ml (15%), and 146.99 µg/ml (25%). Sweet Leaf ZnO NPs: IC50 values of 250.88 µg/ml (5%), 264.22 µg/ml (15%), and 197.24 µg/ml (25%). The sunscreen base without ZnO NPs exhibited an IC50 value of 445.22 µg/ml, and ascorbic acid showed a much lower IC50 of 36.766 µg/ml, highlighting its strong antioxidant potential. Among the formulations, the 25% Ceylon Spinach ZnO NPs sunscreen exhibited the highest antioxidant activity, with the lowest IC50 value of 146.99 µg/ml, while the 5% chemically synthesized ZnO NPs sunscreen exhibited the lowest antioxidant activity with the highest IC50 value of 425.92 µg/ml.

Table 2: Sunscreen Antioxidant activity

Sample	5% IC50 (µg/ml)	15% IC50 (µg/ml)	25% IC50 (µg/ml)
Sweet Leaf ZnO NPs Sunscreen	250.88	264.22	197.24
Ceylon Spinach ZnO NPs Sunscreen	240.52	235.69	146.99
Chemically synthesized ZnO NPs Sunscreen	425.92	416.44	276.92

Table 3: Antioxidant activity of Sunscreen base, Market available Sunscreen and Ascorbic acid

Sample	IC50 (µg/ml)
Cream base antioxidant value	445.22
Market available Sunscreen	415.69
Ascorbic Acid	36.76

3.2.3 UV-Vis Spectroscopic Analysis of Sunscreen

The UV-Vis absorbance data across wavelengths ranging from 220 nm to 400 nm were recorded to evaluate the UV protection properties of sunscreen samples containing ZnO nanoparticles (NPs) synthesized from different sources at varying concentrations. A commercially available sunscreen was also included as a reference. The study assessed nine sunscreen samples, which were categorized as: Chemically synthesized ZnO NPs at 5%, 15%, and 25% concentrations, Ceylon Spinach-synthesized ZnO NPs at 5%, 15%, and 25% concentrations, Sweet Leaf-synthesized ZnO NPs at 5%, 15%, and 25% concentrations. Fig. 8. presents the absorbance values of these sunscreen samples across the specified wavelength range. The absorbance spectra of these samples show variations, which were analyzed for UV protection potential. Higher absorbance values generally correspond to better UV absorption and, consequently, better UV protection. Specifically: UVA protection is suggested by higher absorbance values in the 320-400 nm range, UVB protection is indicated by absorbance in the 280-320 nm range. Sunscreen samples with higher ZnO concentrations, particularly the 25% ZnO sample, exhibited greater absorbance in the UVA range (320-400 nm) compared to those with lower concentrations, such as the 5% ZnO sample. Similarly, the sunscreens containing Ceylon Spinach-synthesized ZnO NPs also followed this trend, with higher ZnO concentrations (25%) resulting in increased UV absorbance. However, slight differences in UV absorbance efficiency were observed between the two synthesis methods. Among the samples, the 25% Ceylon Spinach ZnO NPs sunscreen demonstrated the highest UV absorbance, indicating superior UV protection compared to the other samples.

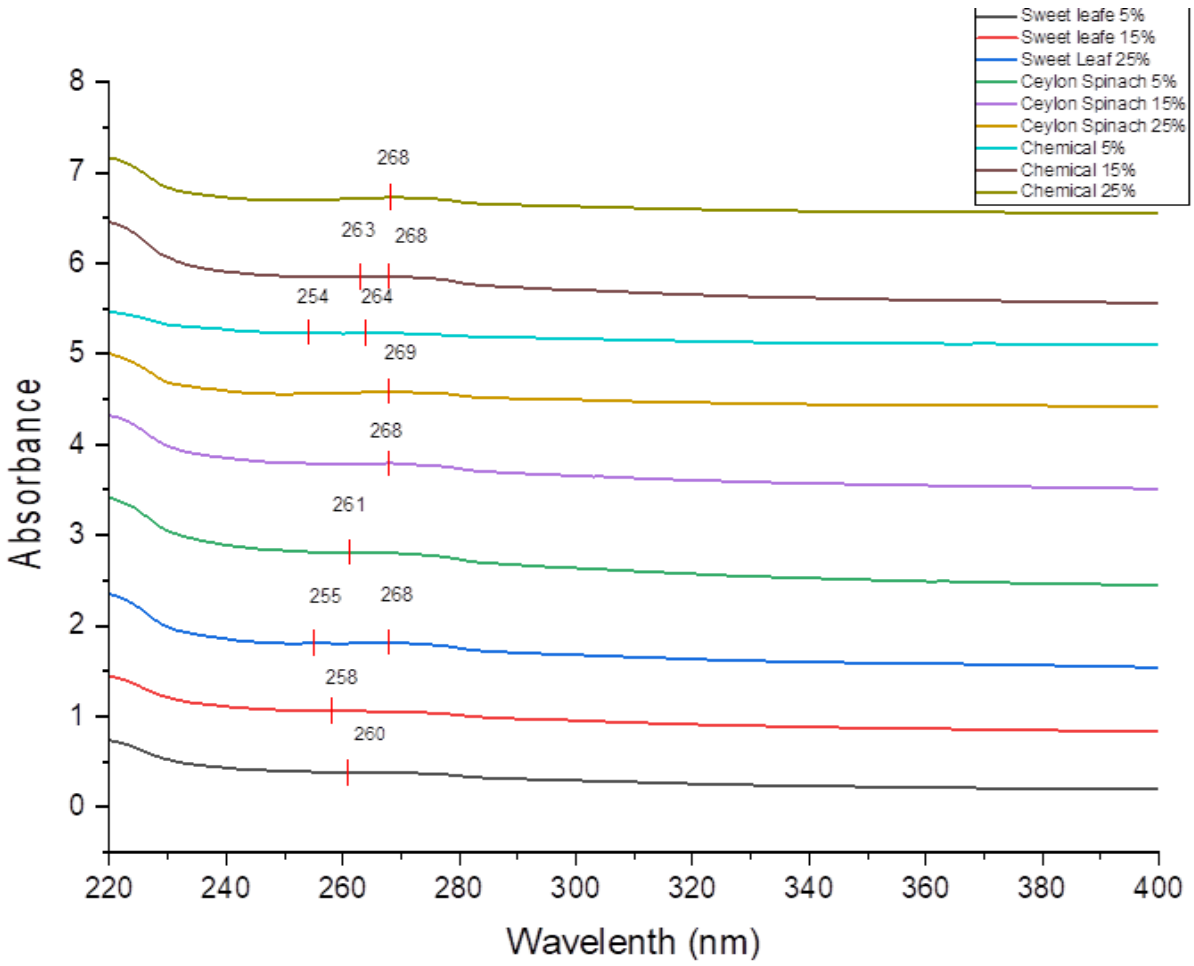

Fig. 8. UV- vis spectrum for Sunscreen samples from different concentrations of chemically and green synthesized ZnO NPs.

3.2.3 Antibacterial Activity of Sunscreen

The antibacterial activity of sunscreens formulated with ZnO nanoparticles synthesized from different sources (chemically synthesized ZnO, Ceylon Spinach ZnO, and Sweet Leaf ZnO) was evaluated against Escherichia coli and Streptococcus aureus strains using the disk diffusion method. Inhibition zone diameters were measured for sunscreens containing 5% and 25% ZnO from each source.

Table 4: Inhibition Zone Diameter (mm) vs. ZnO Source, ZnO Percentage, and Bacterial Strain

ZnO Source	Bacteria Strain		
	ZnO Parentage	*E. coli* (mm)	*S. aureus* (mm)
Chemically synthesized ZnO Sunscreen	5 %	$1.37\pm0.15^{a-d}$	1.17 ± 0.06^{cd}
	25 %	1.33 ± 0.15^{bcd}	1.77 ± 0.25^{a}
Ceylon spinach synthesized ZnO Sunscreen	5 %	1.57 ± 0.21^{abc}	1.27 ± 0.12^{bcd}
	25 %	1.53 ± 0.12^{abc}	1.60 ± 0.20^{ab}
Sweet leaf synthesized ZnO Sunscreen	5 %	1.33 ± 0.12^{bcd}	1.00 ± 0.00^{d}
	25 %	$1.40\pm0.00^{a-d}$	1.53 ± 0.12^{abc}

Note: Values sharing the same letter are not significantly different. $P < 0.05$

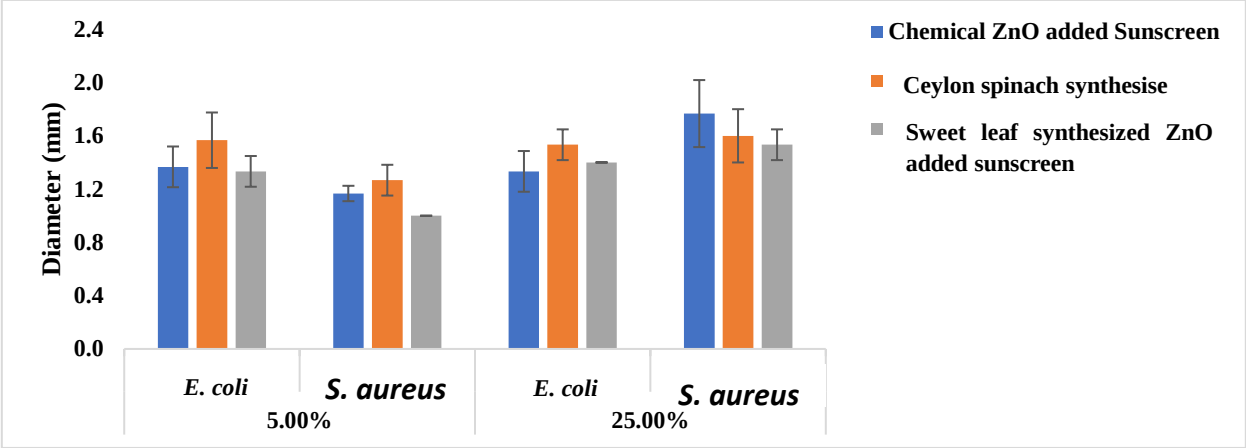

Fig. 9. Bar chart of inhibition zone diameter vs. ZnO source. ZnO percentage and bacteria strain

The interaction between ZnO source, ZnO percentage, and bacterial strain did not show a significant effect on the inhibition zone diameter (p-value = 0.529). However, the Tukey test revealed that the 25% Chemically Synthesized ZnO Sunscreen displayed the largest inhibition zone against S. aureus, while the 5% Sweet Leaf ZnO Sunscreen exhibited the smallest inhibition zone against S. aureus. The main effect of the ZnO source on the inhibition zone diameter was significant (p-value = 0.023). The inhibition zone diameter was higher in sunscreens with Ceylon Spinach ZnO compared to Sweet Leaf ZnO. However, there was no significant difference between Ceylon Spinach ZnO and Chemically Synthesized ZnO sunscreens. In contrast, Sweet Leaf ZnO sunscreens exhibited the smallest inhibition zones, but they were not significantly different from the Chemically Synthesized ZnO sunscreens. The main effect of ZnO concentration on the inhibition zone diameter was highly significant (p-value < 0.0001). In all cases, the inhibition zone diameter for the 25% ZnO samples was significantly larger than for the 5% ZnO samples. The bacterial strain did not significantly influence the inhibition zone diameter (p-value = 0.495), with no significant difference between the inhibition zones for E. coli and S. aureus.

Table 5: Inhibition zone diameter (mm) with selected sample and positive control

Treatment	Sample	Positive control
Chemically synthesized ZnO Sunscreen 25% *S. aureus*	1.77±0.25b	2.60±0.10a
From Ceylon spinach synthesized ZnO Sunscreen 25% *S. aureus*	1.60±0.20b	2.77±0.06a
From Ceylon spinach synthesized ZnO Sunscreen 5% *E. Coli*	1.57±0.21b	2.77±0.12a
From Ceylon spinach synthesized ZnO Sunscreen 25.00% *E. Coli*	1.53±0.12b	2.83±0.12a

Note: Values sharing the same letter are not significantly different. P < 0.05.

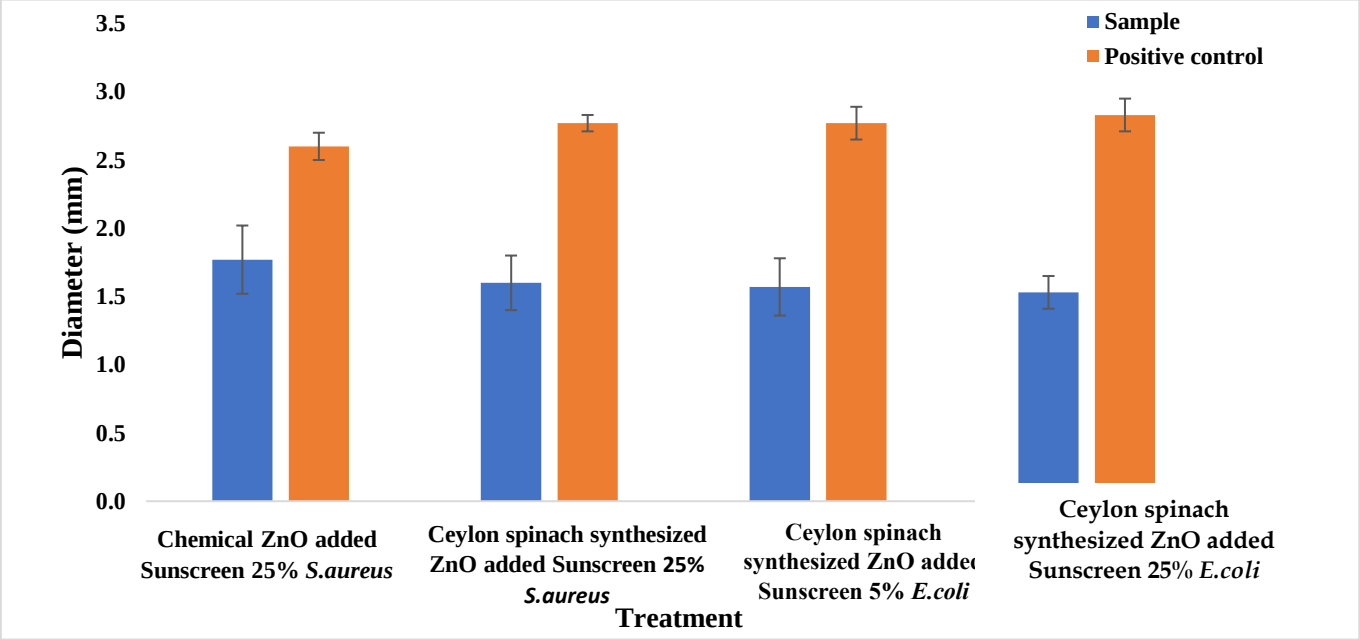

Fig. 10. Bar chart of inhibition zone diameter with selected sample and positive control

Independent sample T-tests indicated that all selected samples exhibited significantly smaller inhibition zones than the relevant positive control, suggesting the antibacterial activity of the ZnO-sunscreen formulations was lower than that of the positive control.

Best product for *E. coli*

Table 6: Inhibition Zone Diameter for *E. coli* Treatment

Treatment	Inhibition zone diameter (mm)
Ceylon spinach synthesized ZnO Sunscreen 5% *E. coli*	1.57±0.21a
Ceylon spinach synthesized ZnO Sunscreen 25% *E. coli*	1.53±0.12a
Market-available sun cream	1.70±0.20a
Cream Base	0.33±0.21b

Note: Values sharing the same letter are not significantly different. $P < 0.05$.

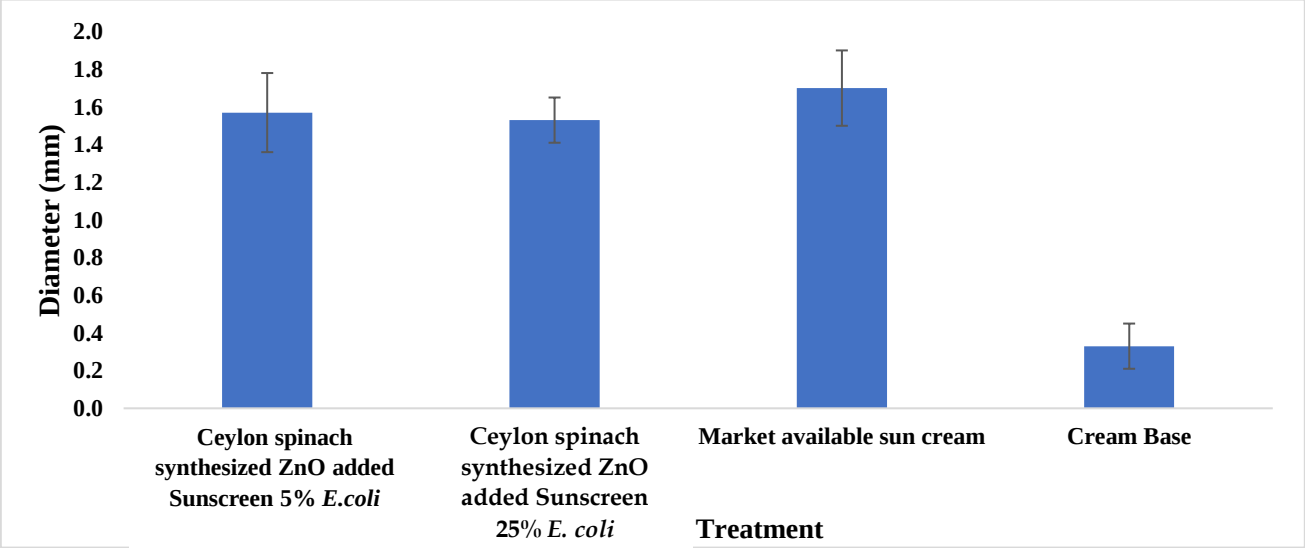

Fig. 11. Bar chart of inhibition zone diameter treatment for *E. coli*

The Tukey test revealed that there was no significant difference between Market-Available Sunscreen, Ceylon Spinach ZnO Sunscreen (5% and 25%), and Ceylon Spinach Synthesized ZnO Sunscreens. The inhibition zone for Cream Base was significantly smaller than the other treatments.

Best product for *S. aureus*

Table 7: Inhibition Zone Diameter for *S. aureus* Treatment

Treatment	Inhibition zone diameter (mm)
Chemically synthesized ZnO Sunscreen 25% *S. aureus*	1.77±0.25a
Ceylon spinach synthesized ZnO Sunscreen 25%	1.60±0.20a
Market-available sun cream	1.60±0.10a
Cream Base	0.40±0.20b

Note: Values sharing the same letter are not significantly different. $P < 0.05$.

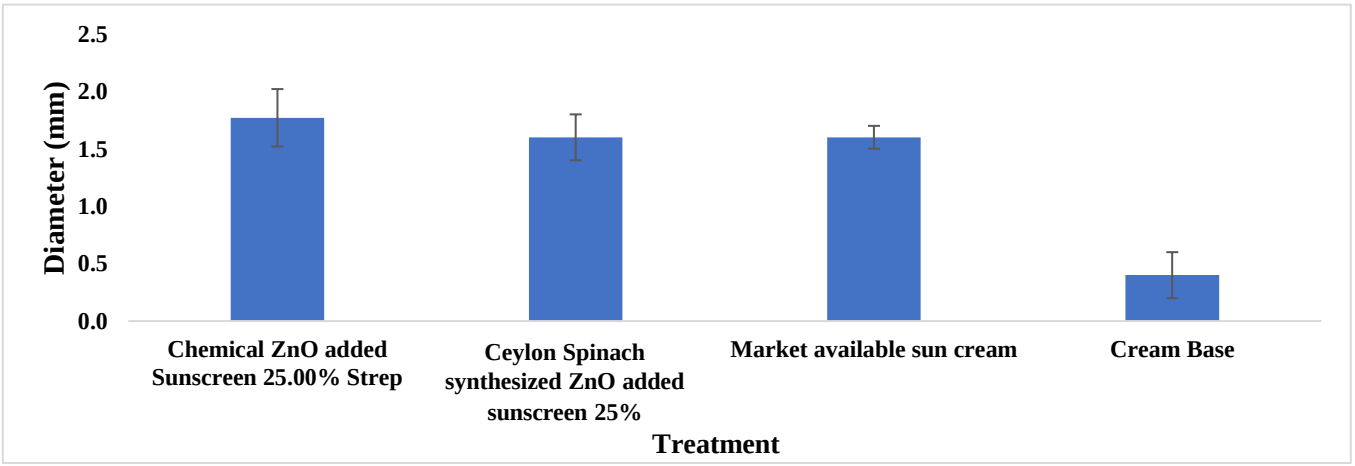

Fig. 12. Bar chart of inhibition zone diameter treatment for *S. aureus*

Tukey's test revealed that there was no significant difference between Chemically Synthesized ZnO Sunscreen (25%), Market-Available Sunscreen, and Ceylon Spinach Synthesized ZnO Sunscreen (25%). However, the inhibition zone for Cream Base was significantly smaller.

CONCLUSION

This study demonstrates the successful application of green synthesis methods for producing Zinc Oxide (ZnO) nanoparticles using Ceylon Spinach and Sweet Leaf extracts, highlighting their potential as an alternative to conventional chemical synthesis in sunscreen formulations. The XRD analysis confirmed the crystalline nature of both chemically and green-synthesized ZnO NPs, while the FTIR analysis indicated the presence of functional groups on the nanoparticle surfaces, contributing to their stability and potential biological interactions. Additionally, the UV-Vis analysis revealed that the green-synthesized ZnO NPs had superior UV absorption properties compared to the chemically synthesized counterparts, further emphasizing their effectiveness in sunscreen applications. Among the various formulations, Ceylon Spinach-synthesized ZnO Sunscreen at 25% concentration stood out as the best antibacterial sample, exhibiting the highest inhibition zone diameter for both *E. coli* and *S. aureus*, making it a promising candidate for microbial protection. Furthermore, the biosynthesized ZnO nanoparticles demonstrated outstanding UV-blocking capabilities, offering effective protection against both UVA and UVB rays, comparable to their chemically synthesized counterparts. The antioxidant and antibacterial activities of these green-synthesized nanoparticles further support their role as multifunctional agents in sunscreen formulations, addressing both UV protection and microbial contamination. Overall, the findings underscore the sustainability and efficacy of green-synthesized ZnO nanoparticles, especially those derived from Ceylon Spinach, as a viable alternative to conventional UV filters. These nanoparticles not only offer improved UV protection but also show enhanced antioxidant and antimicrobial properties, making them a promising eco-friendly option for future sunscreen formulations, with the added benefit of safety and reduced environmental impact.

REFERENCES

[1] S. Zeghoud et al., 'A review on biogenic green synthesis of ZnO nanoparticles by plant biomass and their applications', Dec. 01, 2022, Elsevier Ltd. doi: 10.1016/j.mtcomm.2022.104747.

[2] S. Talam, S. R. Karumuri, and N. Gunnam, 'Synthesis, Characterization, and Spectroscopic Properties of ZnO Nanoparticles', ISRN Nanotechnology, vol. 2012, pp. 1–6, May 2012, doi: 10.5402/2012/372505.

[3] S. Nayak and B. Vaidhun, 'A review of zinc oxide nanoparticles: an evaluation of their synthesis, characterization and ameliorative properties for use in the food, pharmaceutical and cosmetic industries', 2021. [Online]. Available: https://www.researchgate.net/publication/351371482

[4] S. Chandra, S. Singh, and D. Kumari, 'Evaluation of functional properties of composite flours and sensorial attributes of composite flour biscuits', J Food Sci Technol, vol. 52, no. 6, pp. 3681–3688, Jun. 2015, doi: 10.1007/s13197-014-1427-2.

[5] J. Namukobe et al., 'Antibacterial, antioxidant, and sun protection potential of selected ethno medicinal plants used for skin infections in Uganda', Trop Med Health, vol. 49, no. 1, Dec. 2021, doi: 10.1186/s41182-021-00342-y.

[6] H. Agarwal, S. Venkat Kumar, and S. Rajeshkumar, 'A review on green synthesis of zinc oxide nanoparticles – An eco-friendly approach', *Resource-Efficient Technologies*, vol. 3, no. 4, pp. 406–413, Dec. 2017, doi: 10.1016/j.reffit.2017.03.002.

[7] S. W. Balogun, O. O. James, Y. K. Sanusi, and O. H. Olayinka, 'Green synthesis and characterization of zinc oxide nanoparticles using bashful (Mimosa pudica), leaf extract: a precursor for organic electronics applications', *SN Appl Sci*, vol. 2, no. 3, Mar. 2020, doi: 10.1007/s42452-020-2127-3.

[8] H. Bunawan, S. N. Bunawan, S. N. Baharum, and N. M. Noor, 'Sauropus androgynus (L.) Merr. Induced Bronchiolitis Obliterans: From Botanical Studies to Toxicology', 2015, *Hindawi Limited*. doi: 10.1155/2015/714158.

[9] E. K. Droepenu, B. S. Wee, S. F. Chin, K. Y. Kok, and M. F. Maligan, 'Zinc oxide nanoparticles synthesis methods and its effect on morphology: A review', Jun. 15, 2022, *AMG Transcend Association*. doi: 10.33263/BRIAC123.42614292.

[10] K. Geoffrey, A. N. Mwangi, and S. M. Maru, 'Sunscreen products: Rationale for use, formulation development and regulatory considerations', Nov. 01, 2019, *Elsevier B.V.* doi: 10.1016/j.jsps.2019.08.003.

[11] F. Islam *et al.*, 'Exploring the Journey of Zinc Oxide Nanoparticles (ZnO-NPs) toward Biomedical Applications', Mar. 01, 2022, *MDPI*. doi: 10.3390/ma15062160.

[12] A. Jesus *et al.*, 'Antioxidants in Sunscreens: Which and What For?', *Antioxidants*, vol. 12, no. 1, Jan. 2023, doi: 10.3390/antiox12010138.

[13] S. E. Jin and H. E. Jin, 'Synthesis, characterization, and three-dimensional structure generation of zinc oxide-based nanomedicine for biomedical applications', Nov. 01, 2019, *MDPI AG*. doi: 10.3390/pharmaceutics11110575.

[14] G. A. Kaningini, S. Azizi, H. Nyoni, F. N. Mudau, K. C. Mohale, and M. Maaza, 'Green synthesis and characterization of zinc oxide nanoparticles using bush tea (Athrixia phylicoides DC) natural extract: assessment of the synthesis process.', *F1000Res*, vol. 10, p. 1077, Oct. 2021, doi: 10.12688/f1000research.73272.1.

[15] J. D'Orazio, S. Jarrett, A. Amaro-Ortiz, and T. Scott, 'UV radiation and the skin', 2013, *MDPI AG*. doi: 10.3390/ijms140612222.

[16] F. Fikri and M. T. E. Purnama, 'Pharmacology and phytochemistry overview on sauropus androgynous', *Systematic Reviews in Pharmacy*, vol. 11, no. 6, pp. 124–128, 2020, doi: 10.31838/srp.2020.6.20.

[17] K. Geoffrey, A. N. Mwangi, and S. M. Maru, 'Sunscreen products: Rationale for use, formulation development and regulatory considerations', Nov. 01, 2019, *Elsevier B.V.* doi: 10.1016/j.jsps.2019.08.003.

[18] K. Manikandan, T. Balaji, and V. Dhanushkodi, 'Talinum fruticosum: A Potential Multi-value Plant: A Review', *Agricultural Reviews*, no. Of, Sep. 2023, doi: 10.18805/ag.r-2611.

[19] Y. Matsumura and H. N. Ananthaswamy, 'Toxic effects of ultraviolet radiation on the skin', Mar. 15, 2004. doi: 10.1016/j.taap.2003.08.019.

[20] D. Swain, B. Kumar Sahoo, A. Pattanaik, S. K. Mahapatra, and G. Ranjan Rout, 'Pharmacological and biotechnological overview of Sauropus androgynus L. Merr.: an underexploited perennial shrub', 2024. [Online]. Available: http://creativecommons.org/licenses/by-nc-sa/3.0/

[21] T. Kariyawasam, I. Kamani Hewavitharana, T. D. Kariyawasam, and I. K. Hewavitharana, 'Production of plant-derived banana ripening spray using Kappetiya leaves (Croton laccifer)', 2023. [Online]. Available: https://www.researchgate.net/publication/376812657

[22] H. Sampath and I. Kamani Hewavitharana, 'Evaluation of Anthocyanin Extracted from Hibiscus rosa sinensis as a Natural Food Colorant'. [Online]. Available: https://www.researchgate.net/publication/361308508